

Temporal Image Registration using deep learning for 3D Fetal Echocardiography

Kazi Saeed Alam

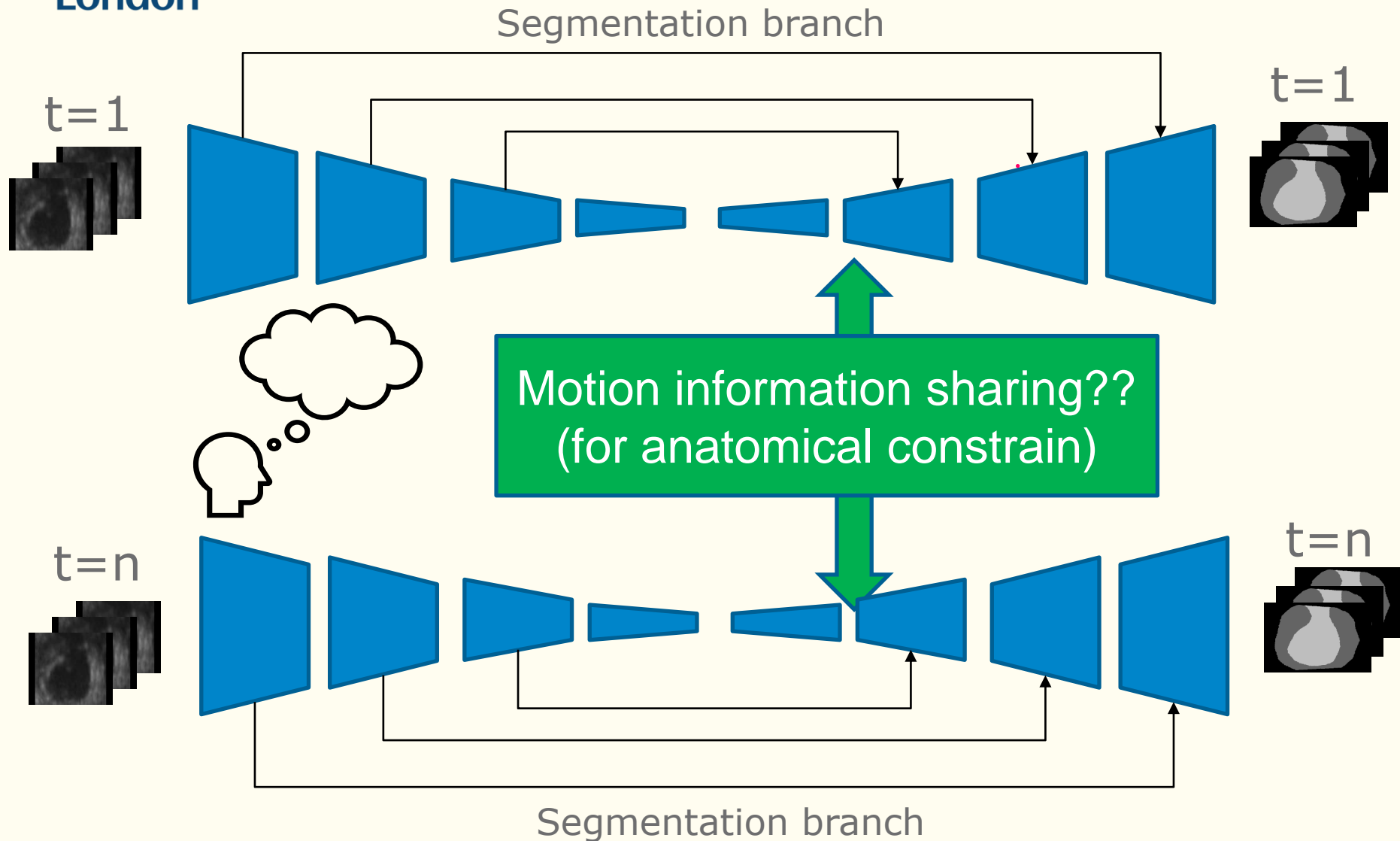
Supervisors: Md Kamrul Hasan,
Dr Choon Hwai Yap

Department of Bioengineering,
Imperial College London, UK

- ① Introduction
 - ① State of the Art
 - ① Dataset description
 - ① Proposed Registration Framework
 - ① Results
 - ① Conclusion & Future Remarks
 - ① References
-

- ⌚ The **fetal heart** can experience congenital heart malformation and functional abnormalities.
- ⌚ **Ultrasound imaging** plays a vital role in assessing the heart of the developing fetus due to its non-invasive nature.
- ⌚ Heart chambers, valves, blood flow patterns, etc. can be used as good **identifiers** to detect and evaluate several cardiac diseases.
- ⌚ However, the detection of heart problems in fetus via mass screening is only around **50%**
- ⌚ The clinical use of echo is still stuck with **2D**
- ⌚ Most of the works are based on **adult hearts**

Temporal Image Registration



The estimation of the **deformation field** by registration between two time points can help share the information between two segmentation branches [1][2][3].

[1] Gupta, Soumya, et al. "Multi-class motion-based semantic segmentation for ureteroscopy and laser lithotripsy." *Computerized Medical Imaging and Graphics* 101 (2022): 102112.

[2] Gupta, Soumya, et al. "Mi-unet: Improved segmentation in ureteroscopy." 2020 IEEE 17th International Symposium on Biomedical Imaging (ISBI). IEEE, 2020.

[3] Xue, Wufeng, et al. "Improved Segmentation of Echocardiography With Orientation-Congruency of Optical Flow and Motion-Enhanced Segmentation." *IEEE Journal of Biomedical and Health Informatics* 26.12 (2022): 6105-6115.

- Public Dataset for 3D echocardiography is very **rare**.
- 2 very well known public datasets are:
 - **CAMUS** [5] :
 - the largest publicly-available and fully-annotated
 - Limitations: data is **2D** and from **adult hearts**
 - **CETUS** [14] : 45 **3D** echocardiographic sequences
 - Adult hearts
 - Nurmaini et. Al. [13] worked on a private dataset of 1149 **2D** images for **fetal** hearts.

State Of the Art (Methods)

*Dice for Intra observer variability **0.930**

Work	Description	Result (Mean Dice Score)
<i>Smistad et al.</i> [15] 2017	<ul style="list-style-type: none"> - used U-Net CNN to segment the left ventricle in 2D ultrasound images. 	0.87 on LV (manual annotated test set)
<i>Oktay et al.</i> [16] 2019	<ul style="list-style-type: none"> - used anatomically constrained neural network (ACNN) segment the 3D LV structure . - Uses segmentation aware maps to add anatomically constraints 	0.912 (ED) and 0.873 (ES) on CETUS dataset
<i>Wei et al.</i> [18] 2020	<ul style="list-style-type: none"> - proposed appearance and shape level co-learning - mutual benefits of the segmentation and tracking 	0.929 for LV and Myo on CAMUS dataset
























State Of the Art (Methods)

*Dice for Intra observer variability **0.930**

Work	Description	Result (Mean Dice Score)
<i>Zhang et al. [18] 2022</i>	<ul style="list-style-type: none"> - dual-branch TransV-Net (DBTV) - V-shaped encoder-decoder branches - extract the additional edge features 	0.913 and 0.880 for left and right ventricle segments on CAMUS Dataset
<i>Sfakianakis et al. [17] 2023</i>	<ul style="list-style-type: none"> - used ensemble of CNNs based on the U-net architecture - Incorporated geometrically constrained data augmentation method based 	0.929 on LV and endocardium on CAMUS Dataset
<i>Ling et al. [19] 2023</i>	<ul style="list-style-type: none"> - proposed four models based on nnUNet (53M parameters) - data augmentation in both training and inference, combined with a well-matched optimization scheme 	0.935 crossing Intra observer variability dice score for LV and myo on CAMUS dataset

Fetal Data Annotation (3D)

**Generate
video
VOL → AVI**

 t1.avi	24/7/2019 10:14 AM	AVI File	52,829 KB	00:00:02
 t2.avi	24/7/2019 10:16 AM	AVI File	52,829 KB	00:00:02
 t3.avi	24/7/2019 10:19 AM	AVI File	52,829 KB	00:00:02
 t4.avi	24/7/2019 10:26 AM	AVI File	52,829 KB	00:00:02
 t5.avi	24/7/2019 10:26 AM	AVI File	52,829 KB	00:00:02
 t6.avi	24/7/2019 10:27 AM	AVI File	52,829 KB	00:00:02
 t7.avi	24/7/2019 10:28 AM	AVI File	52,829 KB	00:00:02
 t8.avi	24/7/2019 10:29 AM	AVI File	52,829 KB	00:00:02
 t9.avi	24/7/2019 10:33 AM	AVI File	52,829 KB	00:00:02
 t10.avi	24/7/2019 10:34 AM	AVI File	52,829 KB	00:00:02
 t11.avi	24/7/2019 10:34 AM	AVI File	52,829 KB	00:00:02
 t12.avi	24/7/2019 10:36 AM	AVI File	52,829 KB	00:00:02
 t13.avi	24/7/2019 10:37 AM	AVI File	52,829 KB	00:00:02
 t14.avi	24/7/2019 10:37 AM	AVI File	52,829 KB	00:00:02
 t15.avi	24/7/2019 10:38 AM	AVI File	52,829 KB	00:00:02
 t16.avi	24/7/2019 10:39 AM	AVI File	52,829 KB	00:00:02
 t17.avi	24/7/2019 10:39 AM	AVI File	52,829 KB	00:00:02
 t18.avi	24/7/2019 10:40 AM	AVI File	52,829 KB	00:00:02
 t19.avi	24/7/2019 10:41 AM	AVI File	52,829 KB	00:00:02
 t20.avi	24/7/2019 10:42 AM	AVI File	52,829 KB	00:00:02
<input type="checkbox"/>  t21.avi	24/7/2019 10:42 AM	AVI File	52,829 KB	00:00:02
 t22.avi	24/7/2019 10:43 AM	AVI File	52,829 KB	00:00:02
 t23.avi	24/7/2019 10:44 AM	AVI File	52,829 KB	00:00:02

Calculate cine at each time point

1. With same **cine length** (adjust start and end slice until cannot see ventricle)
2. **Step size: 0.5mm**
3. Press Start



Generate Slices: AVI to PNG

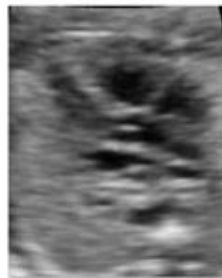
```
Editor - E:\Programming Code\MatlabCode\extract_time.m
extract_time.m generate_fourier_stls.m View_across_time.m +
13 %%%%%%%%% interest
14 %%%%%%%%% - right click within the box and click "crop image"
15
16 bar_dist=10; % gauge bar distance of the two points, chosen to be 10mm
17 TUI_dist=0.5; % please change the TUI dist
18 max_time=36;
19 largest_time=34;
20 video_dir='E:\healthy_fetus_heart_case\01082019';
21
22 Obj=VideoReader([video_dir '\video\' sprintf('t%d.avi',largest_time)]);
23 vid=read(Obj);
```



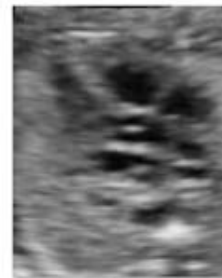
slice019time014.png



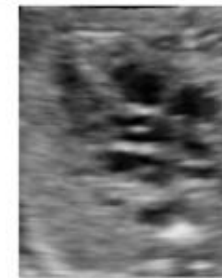
slice020time014.png



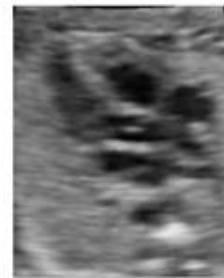
slice021time014.png



slice022time014.png



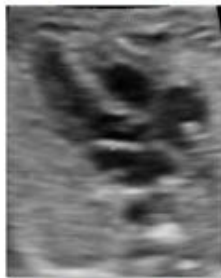
slice023time014.png



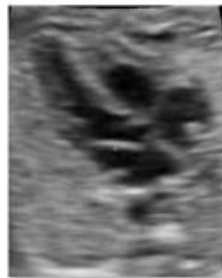
slice024time014.png



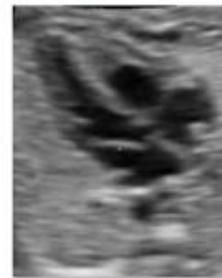
slice025time014.png



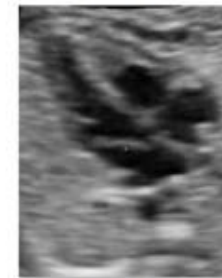
slice026time014.png



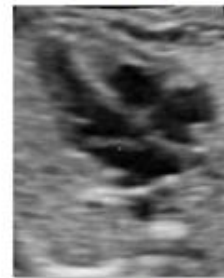
slice027time014.png



slice028time014.png



slice029time014.png



slice030time014.png

Preprocessing

- The ultrasound intensity images contains some artifacts like **constant white boxes** or **arrows**
- **linear interpolation** method was used to remove them
- defected area was interpolated using the intensity values from the **interpolation line**

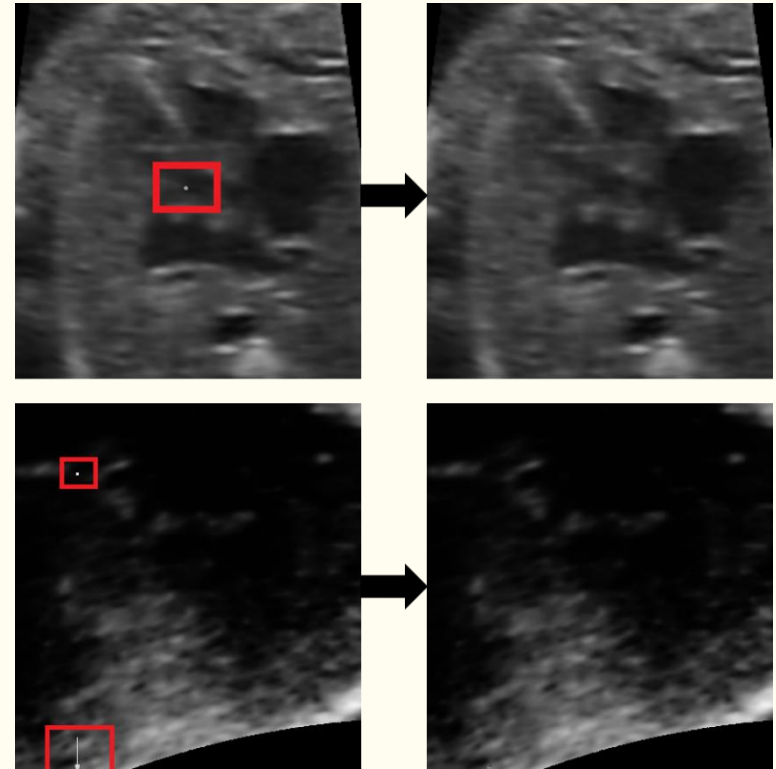


Image Registration

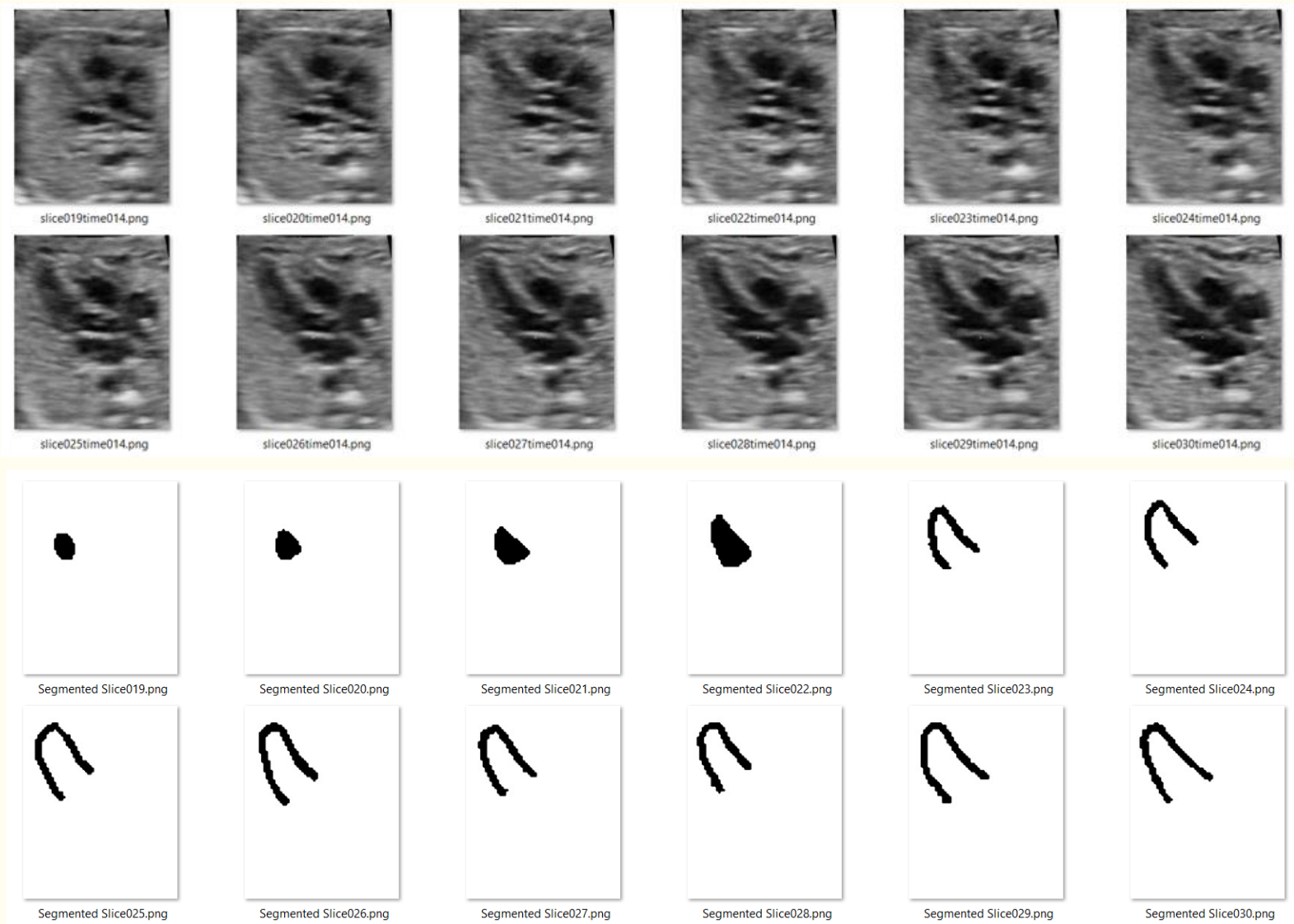
```
(base) E:\healthy_fetus_heart_
medImgProc version 1.0.0
no display found. Using non-ir
Registering t 2 wrt t 1
Registering t 2 wrt t 0
Registering t 3 wrt t 2
Registering t 3 wrt t 0
Registering t 4 wrt t 3
Registering t 4 wrt t 0
Registering t 5 wrt t 4
Registering t 5 wrt t 0
Registering t 6 wrt t 5
Registering t 6 wrt t 0
Registering t 7 wrt t 6
Registering t 7 wrt t 0
Registering t 8 wrt t 7
Registering t 8 wrt t 0
Registering t 9 wrt t 8
```

- Register image with respect to t1 and the previous time point
- Libraries used:
 - **SimpleElastix**
 - **Cardiac motion estimation** library by Wiputra et al. (2020)[1]
[<https://github.com/WeiXuanChan/motionSegmentation>]
- uses the Fourier b-splines spatiotemporal motion model to fit the deformation fields.

Image Segmentation (lazysnap)

```
E:\Programming Code\Lazy Snap Heart.exe
Give the path to the folder where folders containing images are stored :
E:\healthy_fetus_heart_case\01082019
Give the number of Slices:
6
Give the number of Times:
27
Give start time:
27
Give start slice:
6
Give image skip value (default 0, no skip):
0
E:\healthy_fetus_heart_case\01082019\time027\segmented\Segmented Slice006.png
Press 'f'then hold and drag left click to select the foreground region
Press 'b'then hold and drag left click to select the background region
Press 'r' to reset the image segmentation procedure
Press esc to quit and save the images
_
```

- **Two** time points to segment
 1. End-systolic
 2. End-diastolic



3D Reconstruction

- vmtk(Vascular Modeling Toolkit) was used to generate the 3D masks
- Generated 3D masks have artifacts like **holes**, **spikes**, **edges** etc which was corrected and smoothened using Geomagic by an expert.

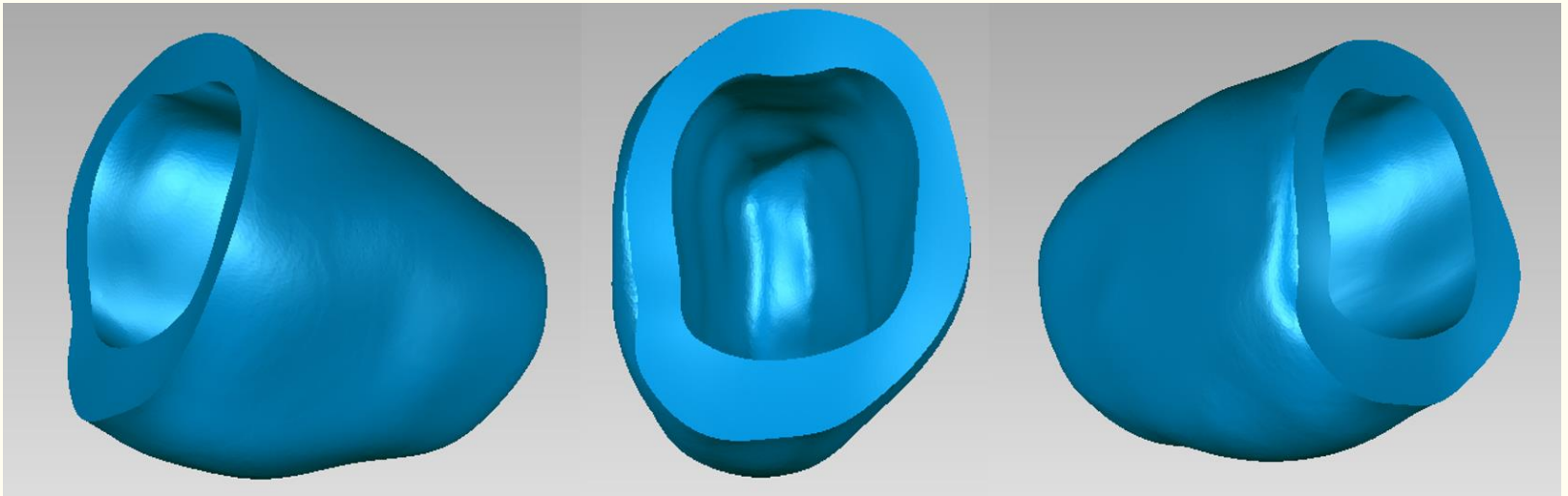
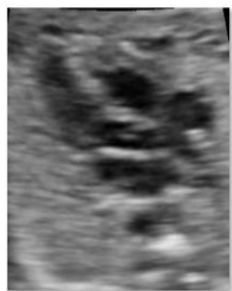
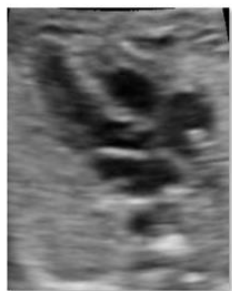


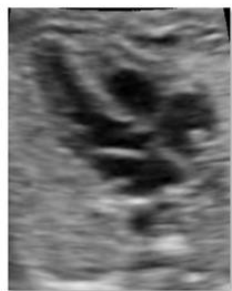
Image-Mask Pair



slice025time014.png



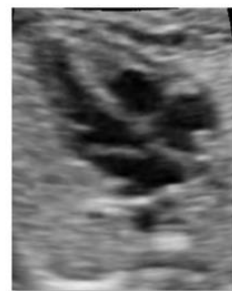
slice026time014.png



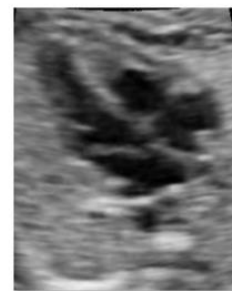
slice027time014.png



slice028time014.png



slice029time014.png



slice030time014.png



Segmented Slice025.png



Segmented Slice026.png



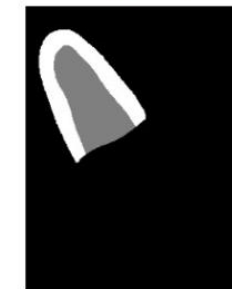
Segmented Slice027.png



Segmented Slice028.png



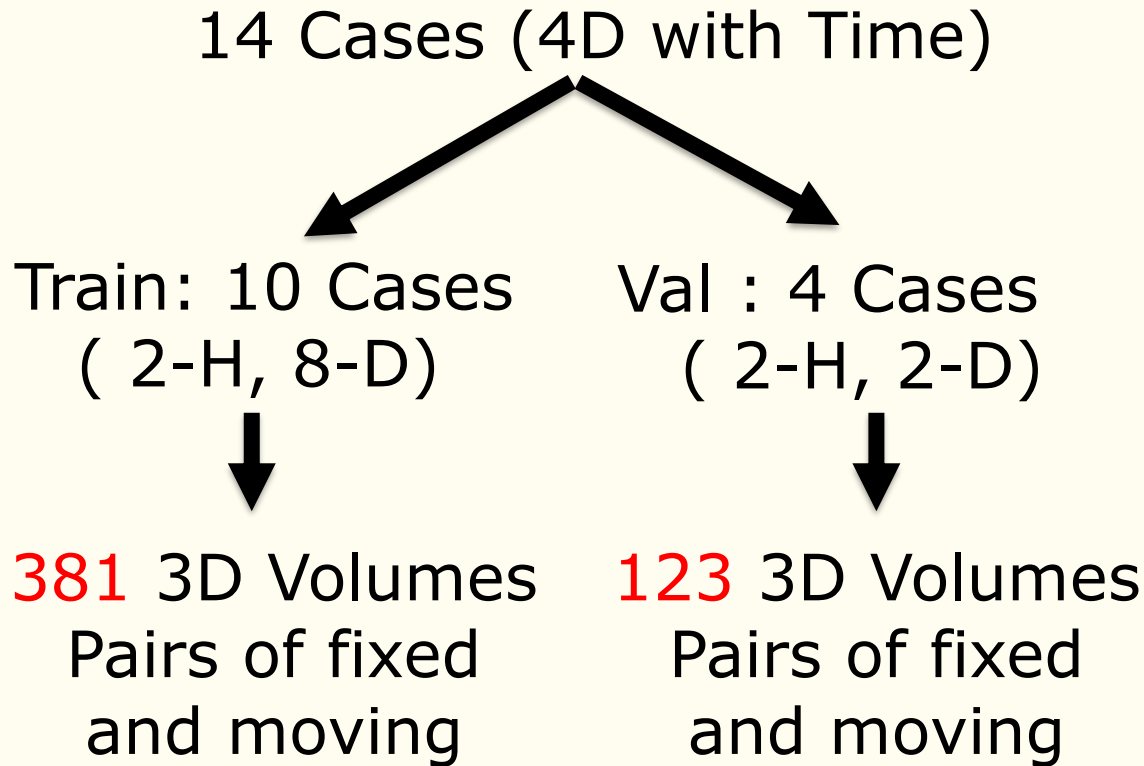
Segmented Slice029.png



Segmented Slice030.png

Fetal 3D Dataset

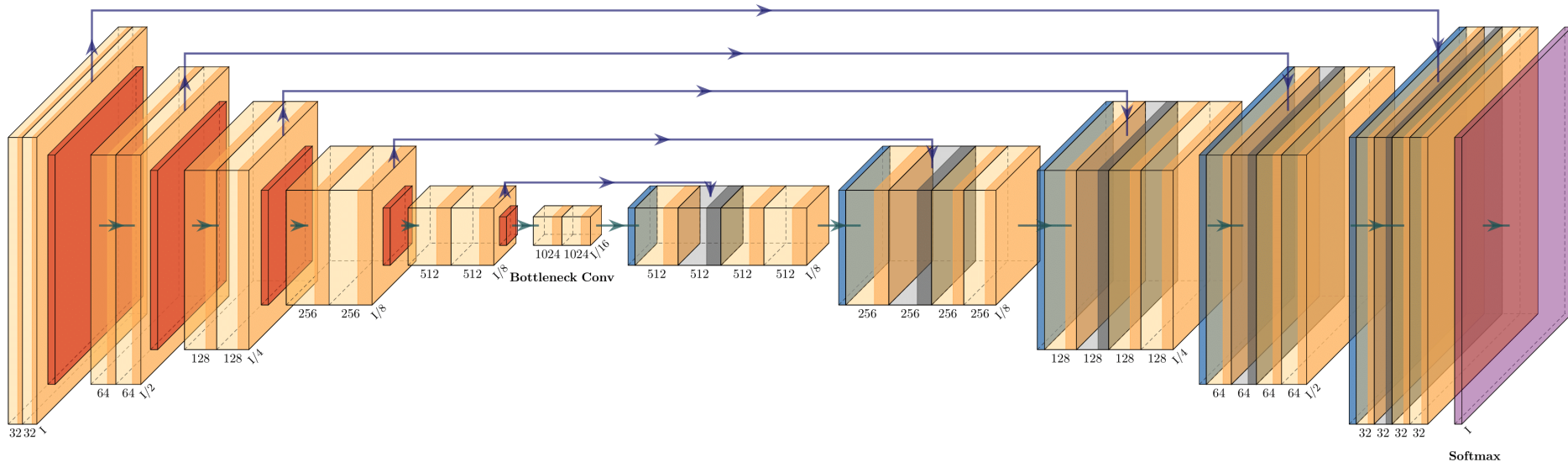
H: Healthy
D: Diseased



- We have also applied our experimental methods on a well-known adult **2D** echocardiography dataset.[5]
- We wanted to compare the performances in **2D vs 3D**
- Also in **adult vs fetal** echocardiography
- CAMUS dataset comprises :
 - i) a training set of **450** patients along with the corresponding manual references;
 - ii) a testing set composed of **50** new patients.

Proposed registration Framework

(1) Proposed Residual Segmentation branch

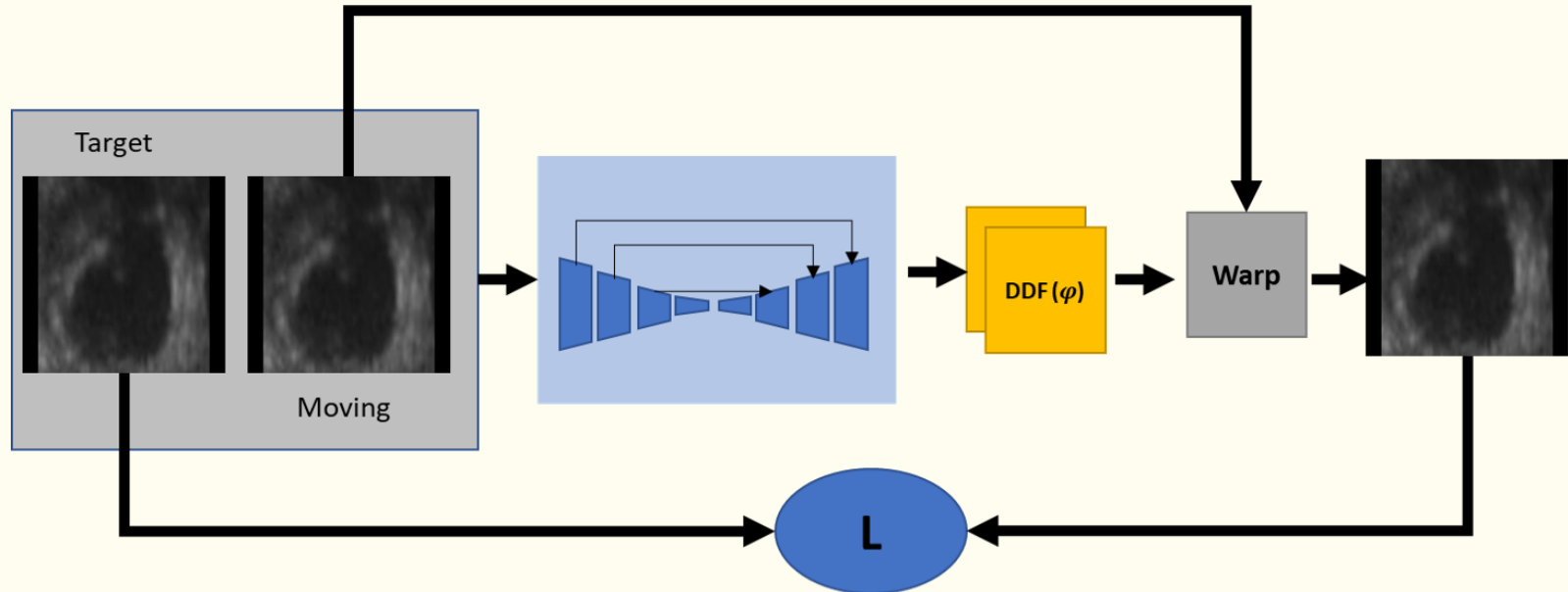


- Based on the traditional **UNET** architecture with skip connections. (Input Image: 256*256*32)
- The conventional path cannot degrade the features' quality as a non-zero regularizing path will skip over them. On the other hand, the direct skipping of the non-zero regularizing path cannot hamper the performance as it has been added to the conventional path's learned features.

(2) Multi-class Anatomically Constrained and multi-scale registration

The proposed registration method has the following integral parts:

1. Local and global anatomical constraints using variational autoencoders
2. Adversarial learning as like zero-sum game theory (one agent's gain is another agent's loss), where the discriminator is used to classify moved and fixed images
3. Multi-scale (multi-resolution) training, where trained parameters in lower scale are used to initialize the higher scale training (Future works for 3D)



Typical unsupervised Registration without considering anatomy.

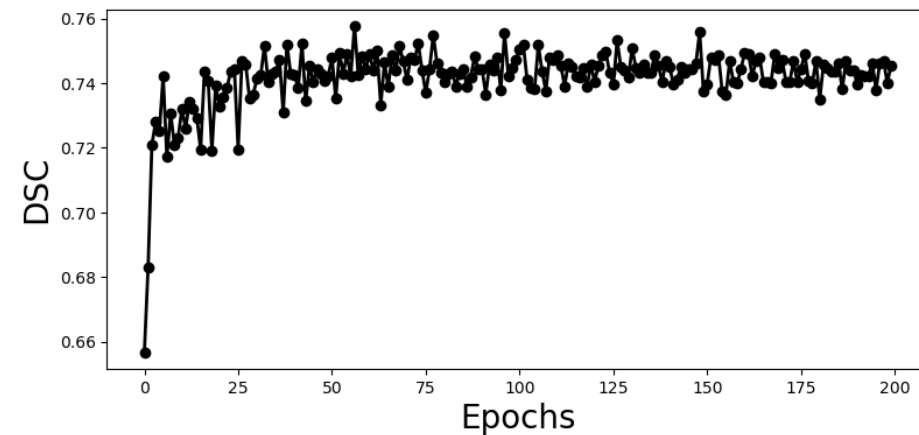
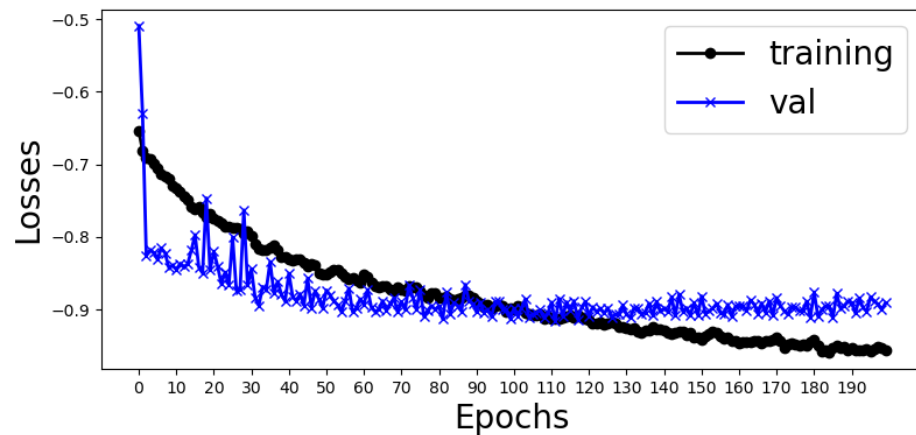
$$\mathcal{L}_{us}(f, m, d) = \mathcal{L}_{sim}(f, m \circ d) + \lambda \mathcal{L}_{smooth}(d)$$

$$MI(f_x; m_y) = \sum_{x \in X} \sum_{y \in Y} P(f_x, m_y) \log_2 \left(\frac{P(f_x, m_y)}{P(f_x)P(m_y)} \right)$$

$$\mathcal{L}_{smooth}(d) = \sum_{\mathbf{d} \in D} \|\nabla \mathbf{u}(\mathbf{d})\|^2$$

- The **unsupervised loss** can be derived using MI loss and binding energy regularization loss

Results on Fetal Dataset (3D) – Longitudinal Registration

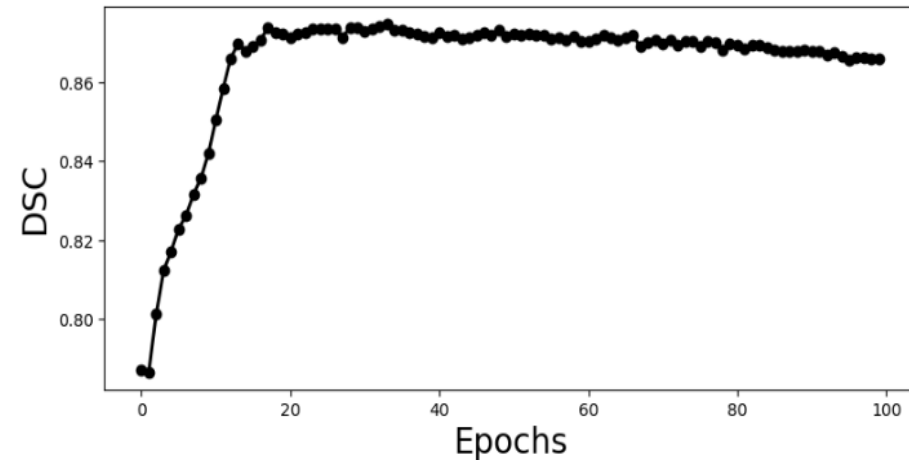
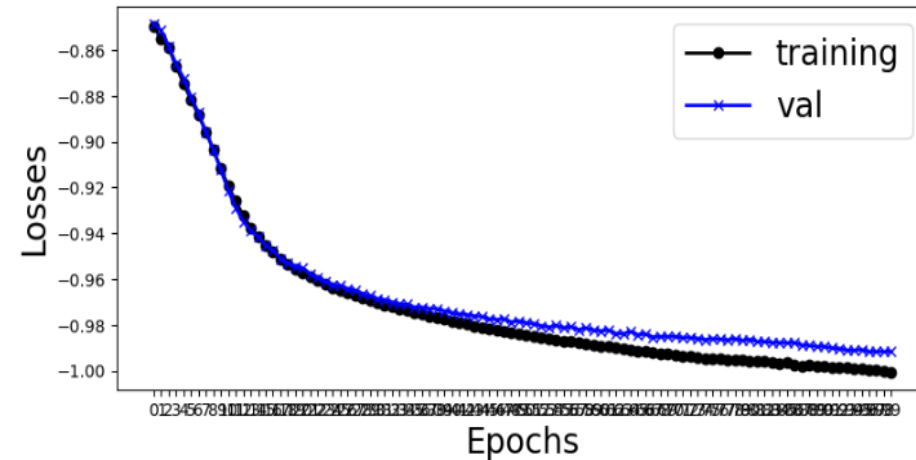


MSEMetric W/O registration = 0.00377

MSEMetric W/ registration = 0.00296

	BG	LV	Myo
Mean dice W/O registration =	0.99093	0.78917	0.72605
Mean dice W/ registration =	0.98699	0.70087	0.58543

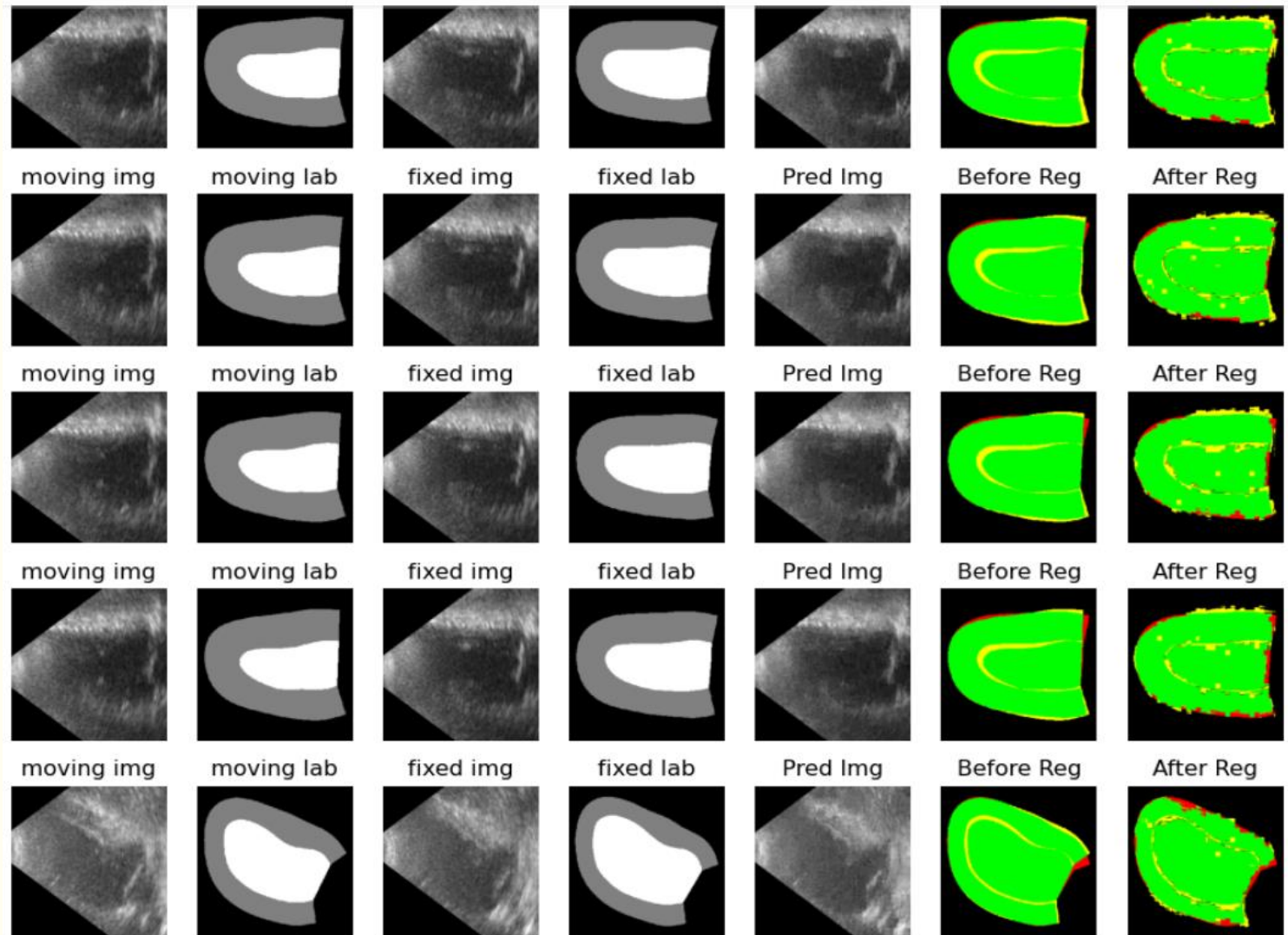
Results on CAMUS Dataset (2D) - Longitudinal Registration



MSEMetric W/O registration = 0.00972

MSEMetric W/ registration = 0.0042

	BG	LV	Myo
Mean dice W/O registration =	[0.96678	0.76046	0.69391]
Mean dice W/ registration =	[0.97352	0.87523	0.74977]



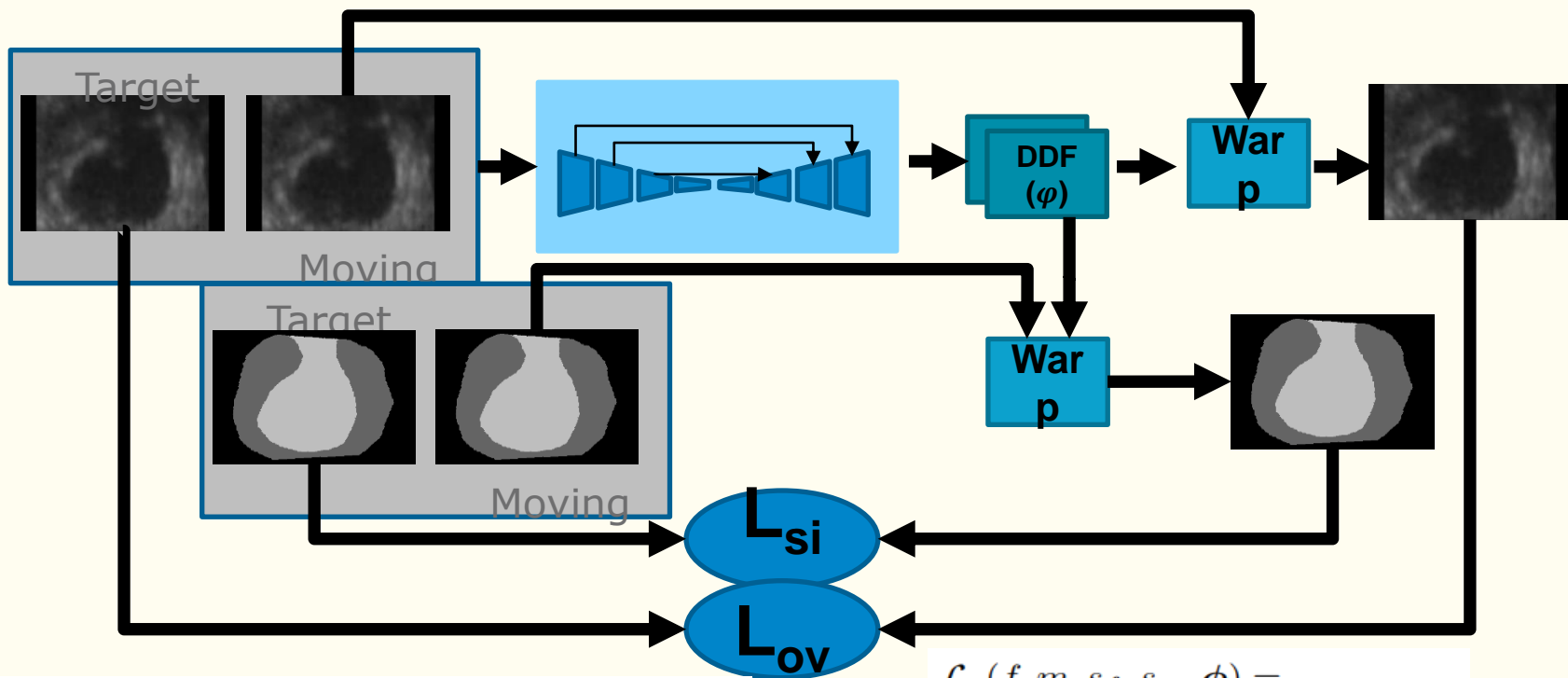
Observation:

- In the unsupervised registration without considering the anatomy, the similarity between two intensity images **increases**, but the similarity between fixed and moved masks does not improve satisfactorily or **fail** in some cases.

Thanks to those two following papers that solved this limitation.

[1] Balakrishnan, Guha, et al. "VoxelMorph: a learning framework for deformable medical image registration." IEEE transactions on medical imaging 38.8 (2019): 1788-1800.

[2] Hu, Yipeng, et al. "Label-driven weakly-supervised learning for multimodal deformable image registration." 2018 IEEE 15th International Symposium on Biomedical Imaging (ISBI 2018). IEEE, 2018.



$$\mathcal{L}_{us}(f, m, \phi) = \mathcal{L}_{sim}(f, m \circ \phi) + \lambda \mathcal{L}_{smooth}(\phi)$$

$$\mathcal{L}_a(f, m, s_f, s_m, \phi) = \mathcal{L}_{us}(f, m, \phi) + \gamma \mathcal{L}_{seg}(s_f, s_m \circ \phi)$$

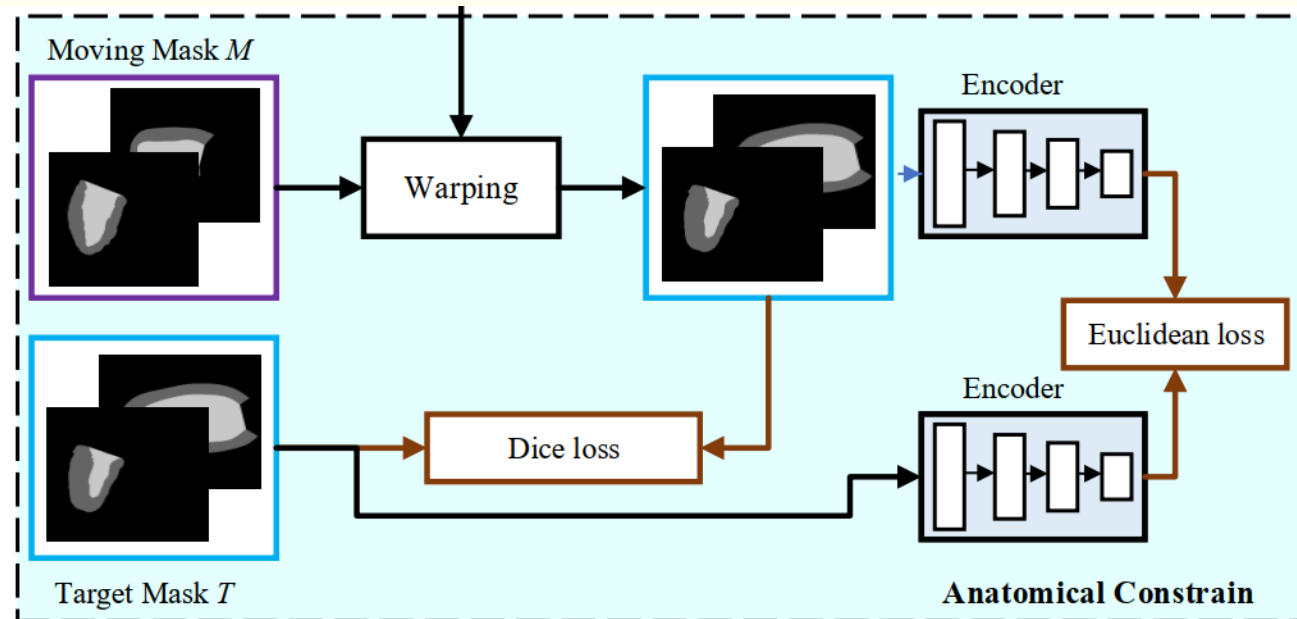
```
# do registration
displacement_field = reg_net(torch.cat((img1,img2), dim=1))

# do segmentation
seg1 = seg_net(img1).softmax(dim=1)
seg2 = seg_net(img2).softmax(dim=1)

# warp segmentation using the same warp block defined above
seg2_warped = warp(seg2, displacement_field)

# compute multiclass dice loss
dice_loss = monai.losses.DiceLoss()
anatomy_loss = dice_loss(seg2_warped, seg1)
```

- \mathcal{L}_{seg} is measured using the **Dice-Loss**.

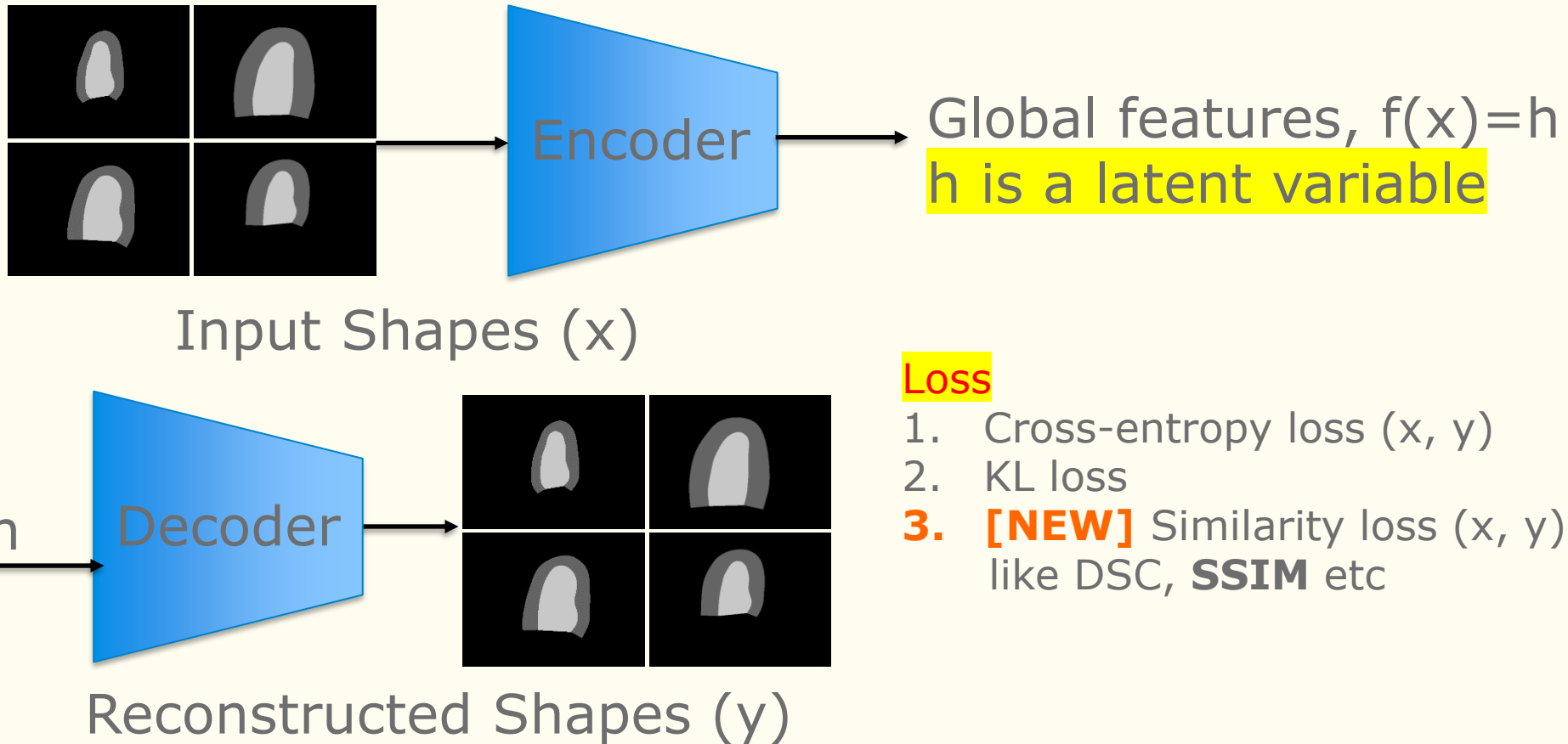


To improve the network's anatomical context:

Intensity-based similarity loss (fixed and moving intensity images) with a segmentation-aware loss (fixed and moved labels) are combined.

This new loss measures the alignment between a target anatomical mask and a warped moving mask.

Learning Global Anatomical Features



The regularization loss named **Kullback-Leibler (KL)** divergence forces the distributions returned by the encoder to be close to a standard normal distribution.

Goal from Global attributes

Orientation, Shape, and Size

Original images



Reconstructed images



Best Val Dice = **0.9789**

Goal from Global attributes

Orientation, Shape, and Size

Original images

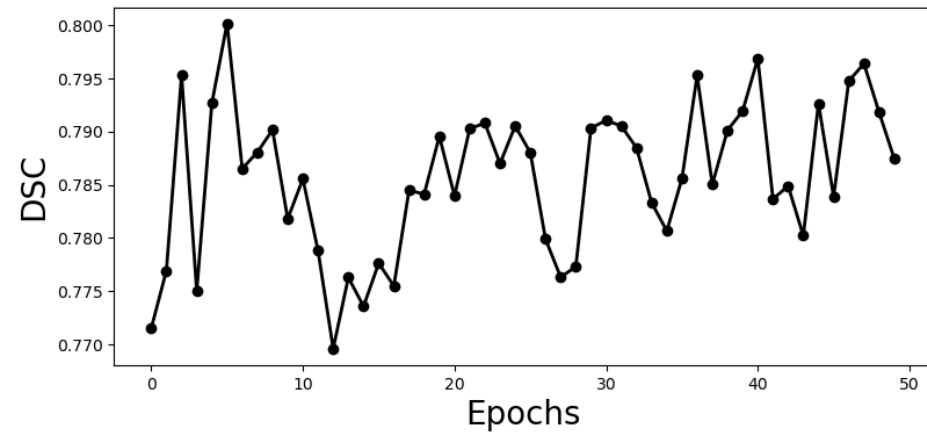
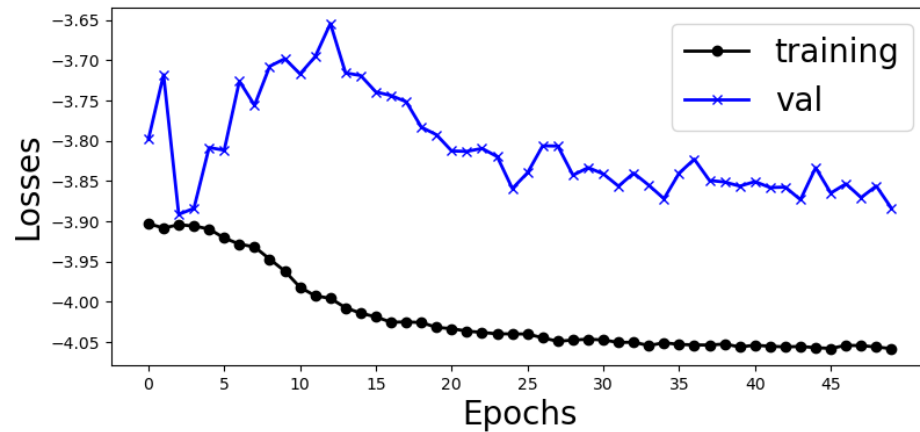


Reconstructed images



Best Val Dice = **0.9407**

Results on Fetal Dataset (3D) – Longitudinal Registration

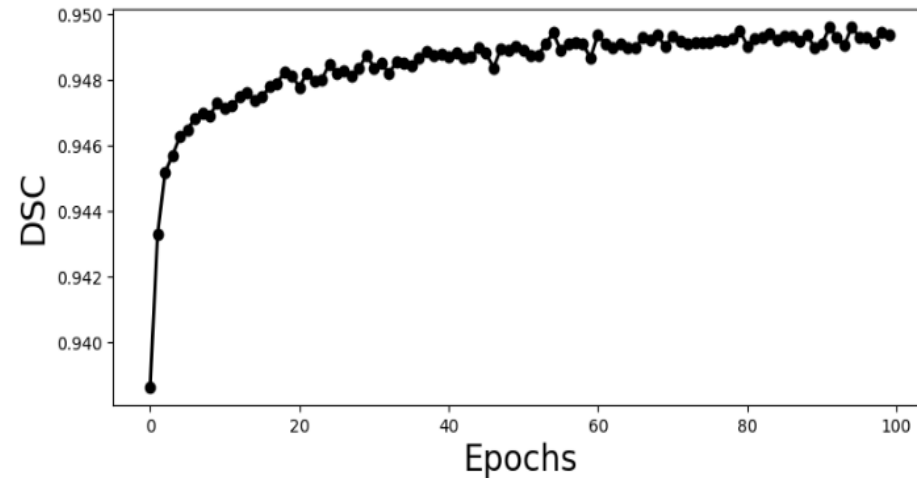
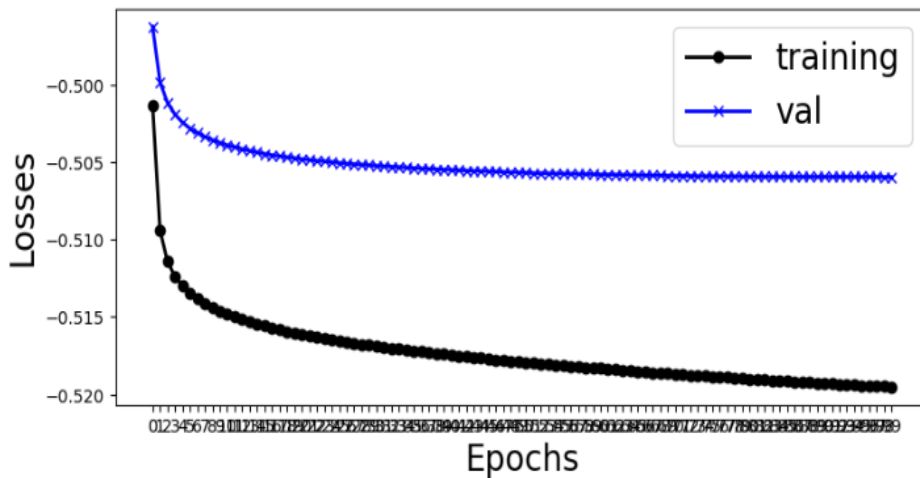


MSEMetric W/O registration = 0.00377

MSEMetric W/ registration = 0.00251

	BG	LV	Myo
Mean dice W/O registration =	0.99093	0.78917	0.72605
Mean dice W/ registration =	0.98959	0.73347	0.64435

Results on CAMUS Dataset (2D) - Longitudinal Registration

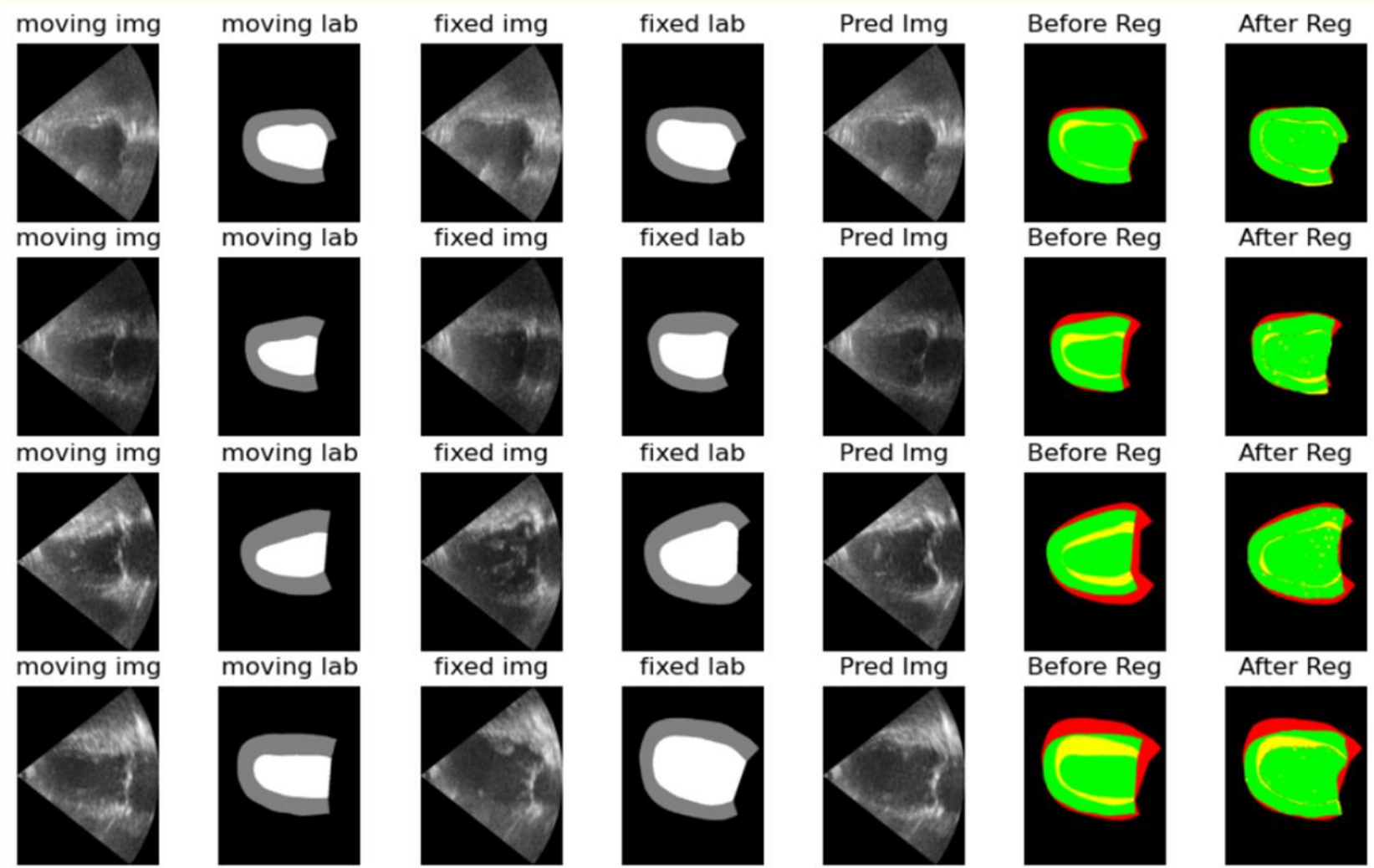


MSEMetric W/O registration = 0.00972

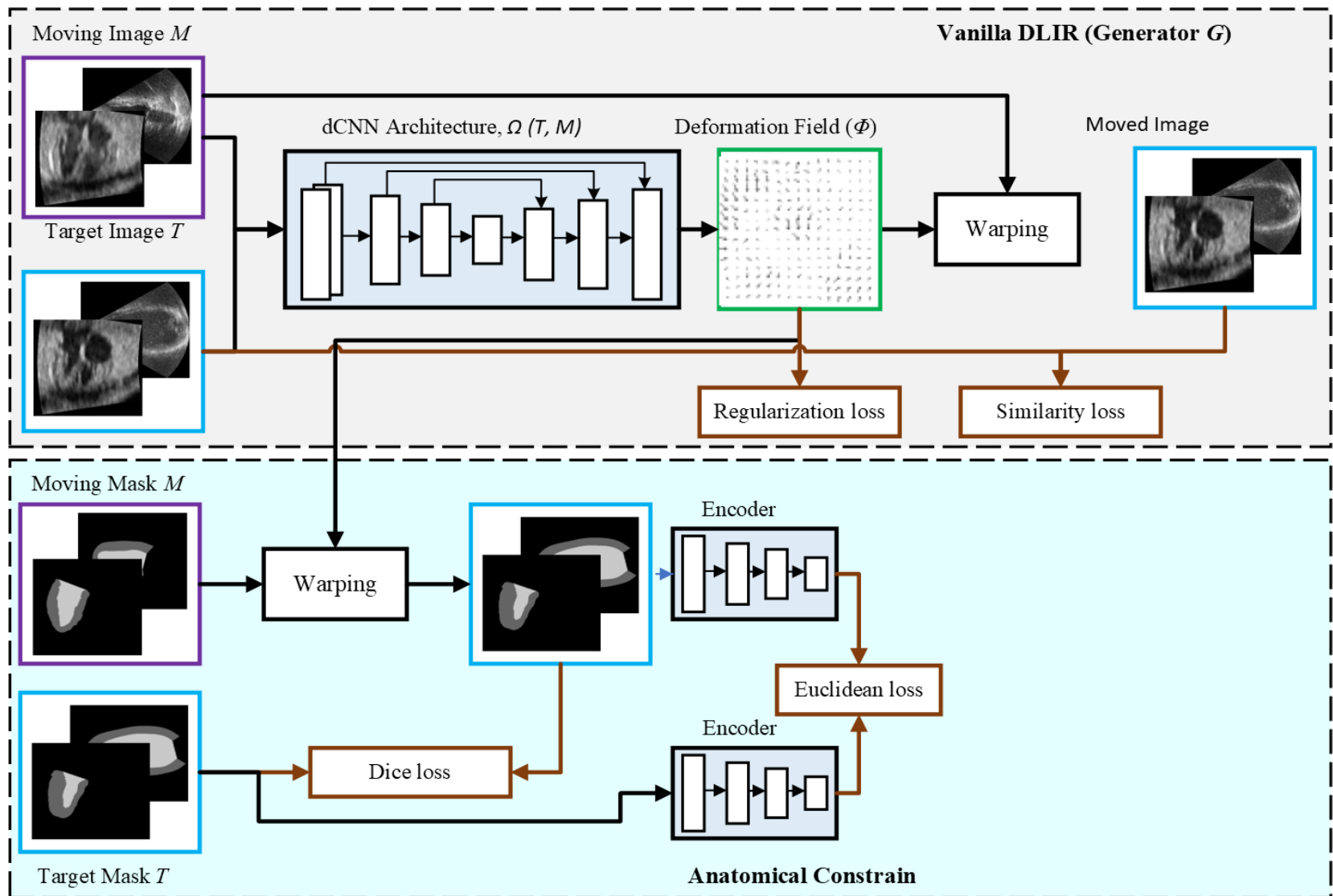
MSEMetric W/ registration = 0.00598

	BG	LV	Myo
Mean dice W/O registration =	[0.96678	0.76046	0.69391]

Mean dice W/ registration =	[0.97972	0.91935	0.81437]
-----------------------------	----------	---------	----------

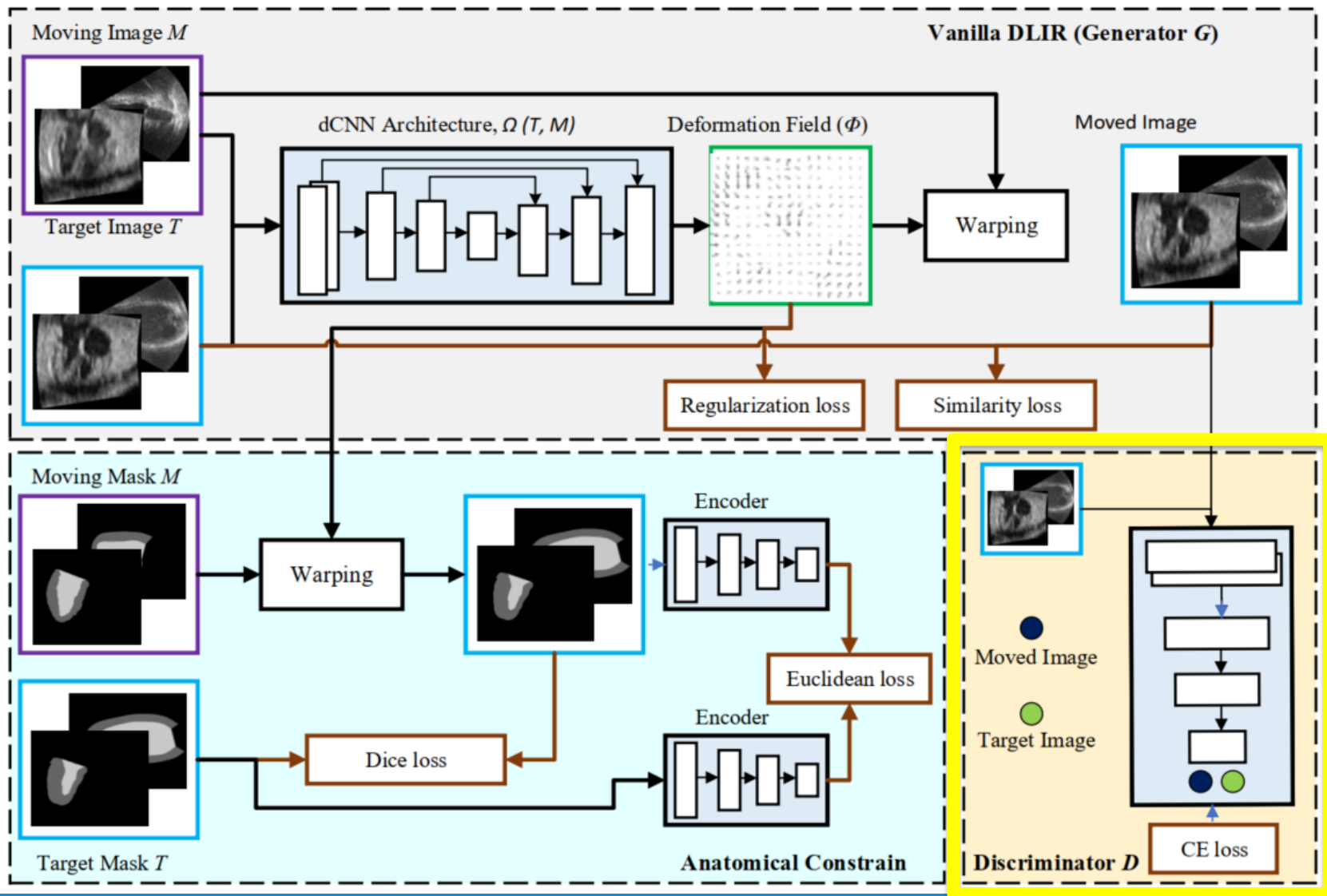


Anatomically constrained DLIR (AC-DLIR)



- Still, there is room for performance improvement.
- Hence, we proposed **Adversarial** Anatomically constrained (AdvAC) DLIR framework.
- The part of AC-DLIR for generating the deformable images as a **generator** for the adversarial network.
- A **discriminator** was also trained which was able to classify the fixed and moved images
- While training, the generator would try to create as much as **plausible images** as the fixed image whereas the discriminator would try to discriminate them.

Adversarial AC-DLIR (AdvAC-DLIR)



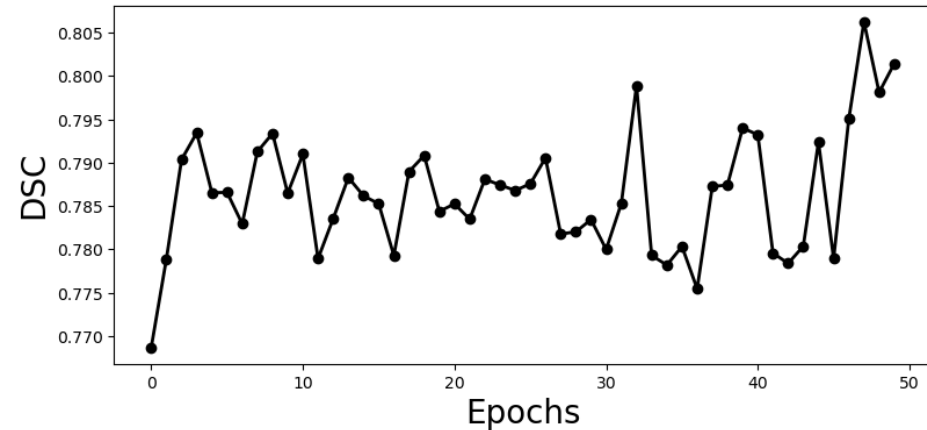
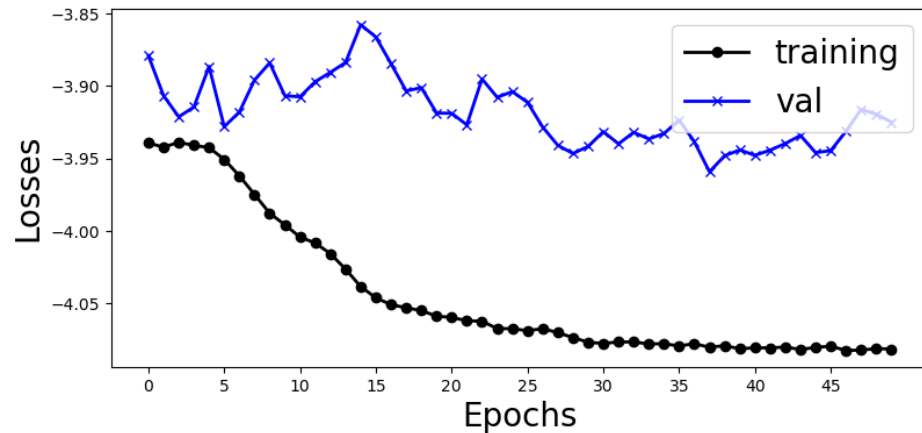
Proposed Loss Functions

$$\mathcal{L}_{advac}(f, m, r_f, r_m, d, s_m) = \mathcal{L}_{us}(f, m, d) + \beta \mathcal{L}_{dice}(r_f, r_m \circ d) \\ + \gamma \mathcal{L}_{L2}(r_f, r_m) + \phi \mathcal{L}_g(m, s_m)$$

Here,

- \mathcal{L}_{us} is the unsupervised loss function coming from Vanilla-DLIR.
- \mathcal{L}_{dice} is the segmentation aware loss
- \mathcal{L}_{L2} is the loss from latent space consideration
- \mathcal{L}_g is the generator's binary cross entropy loss
- and β, γ and ϕ are regularization parameters

Results on Fetal Dataset (3D) – Longitudinal Registration

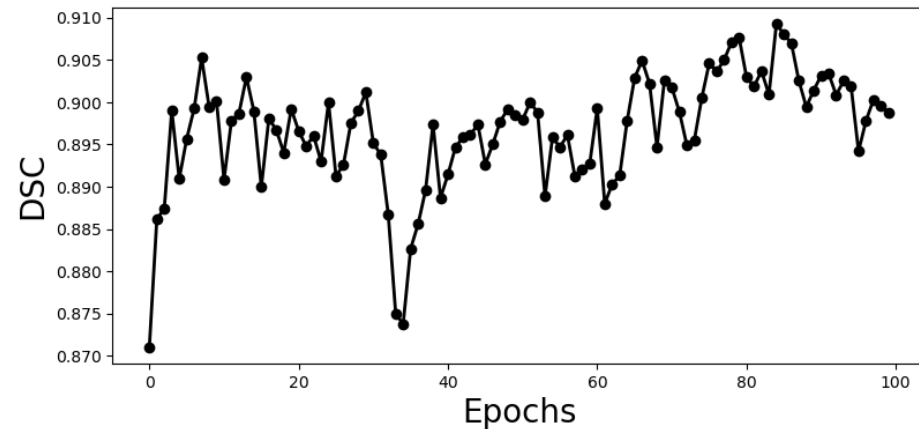
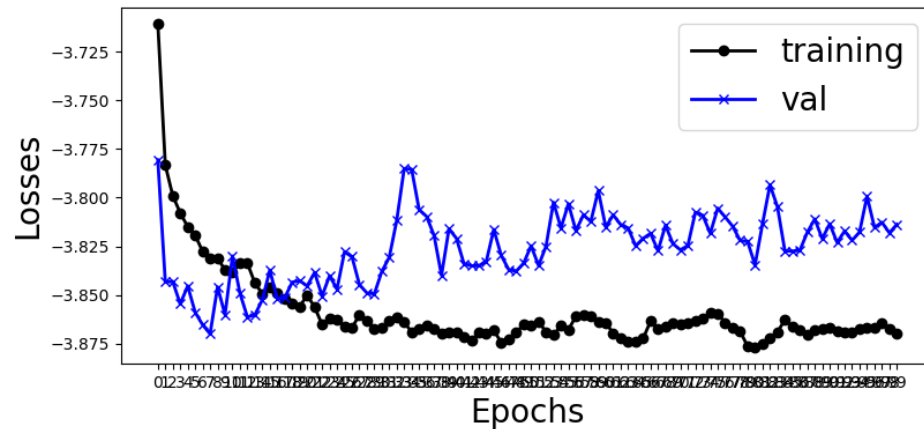


MSEMetric W/O registration = 0.00377

MSEMetric W/ registration = 0.00258

	BG	LV	Myo
Mean dice W/O registration =	0.99093	0.78917	0.72605
Mean dice W/ registration =	0.99089	0.79884	0.73482

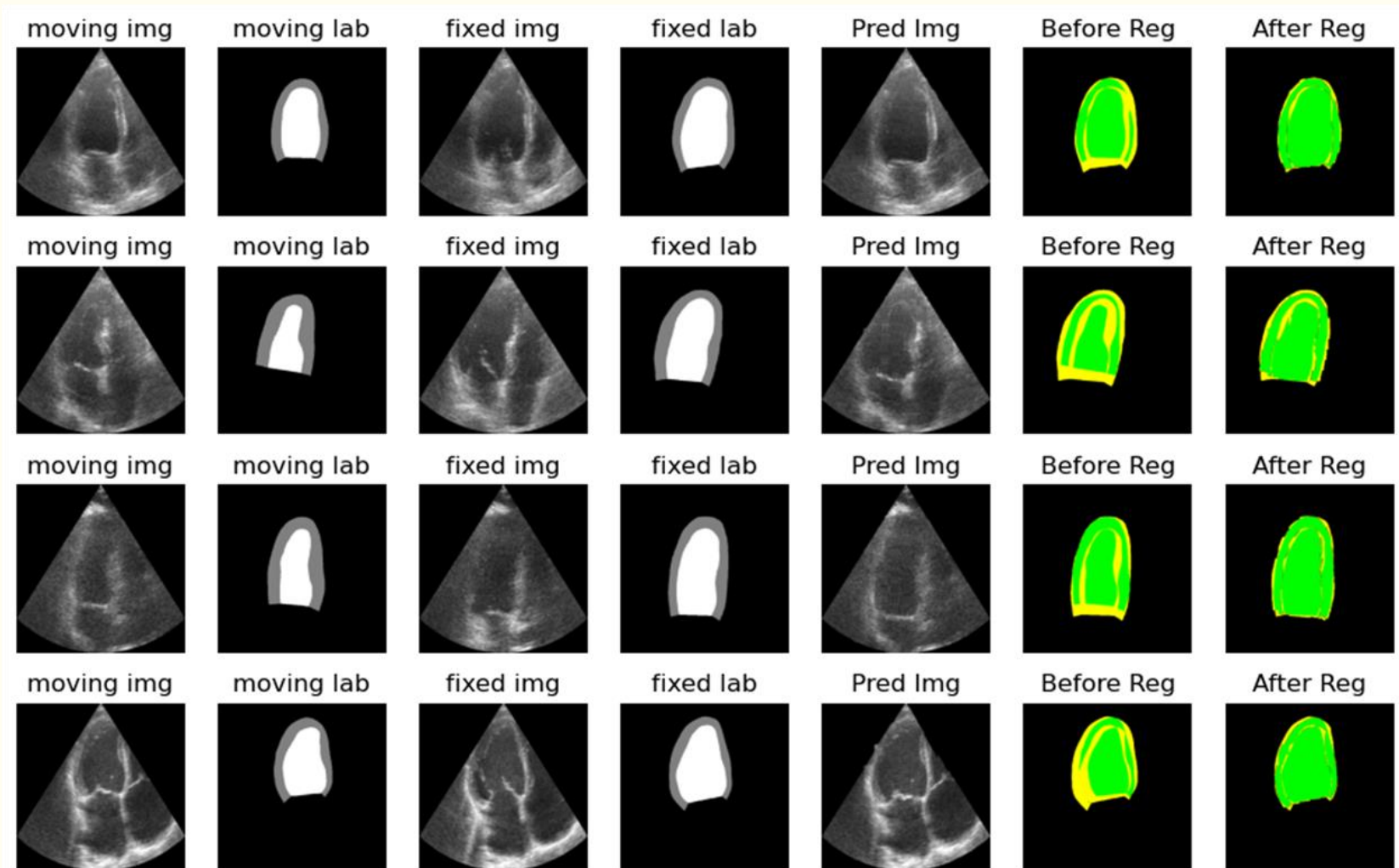
Results on CAMUS Dataset (2D) - Longitudinal Registration



MSEMetric W/O registration = 0.00972

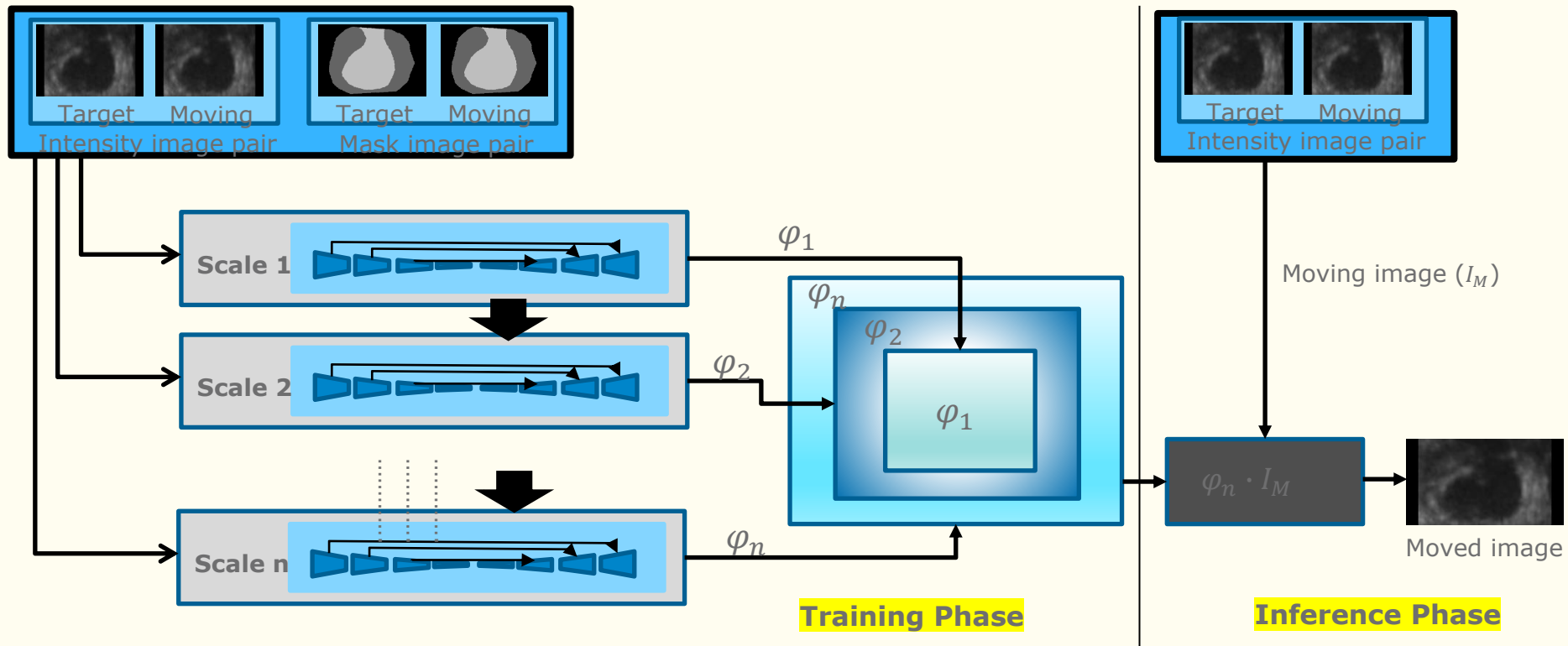
MSEMetric W/ registration = 0.00589

	BG	LV	Myo
Mean dice W/O registration =	[0.96678	0.76046	0.69391]
Mean dice W/ registration =	[0.98742	0.93573	0.82751]

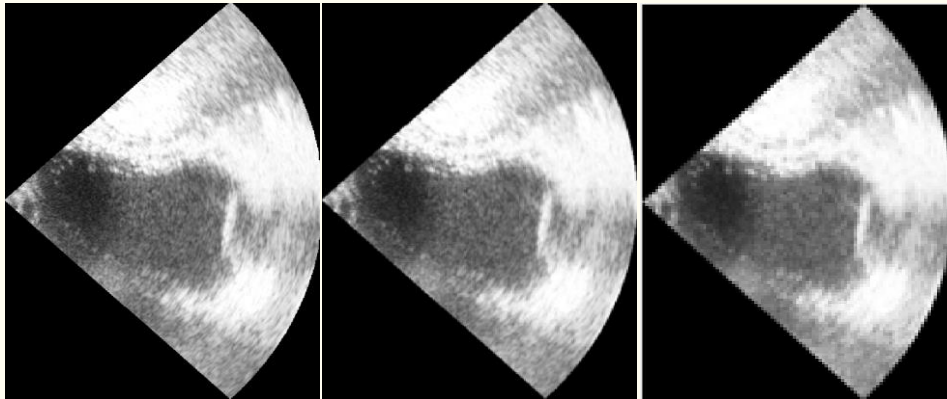


Results (Fetal 3D)

Model	MSE	Dice Score			Mean Dice \pm std
		Background	LV	Myo	
Without Registration	0.00377	0.99093	0.78917	0.72605	0.83539 \pm 0.12798
Vanilla-DLIR	0.00296	0.98699	0.70087	0.58543	0.75776 \pm 0.04036
AC-DLIR	0.00251	0.98959	0.73347	0.64435	0.80013 \pm 0.05401
Adv-DLIR	0.00339	0.99031	0.73836	0.67389	0.80989\pm 0.05142
AdvAC-DLIR	0.00258	0.99089	0.79884	0.73482	0.84668\pm 0.04586



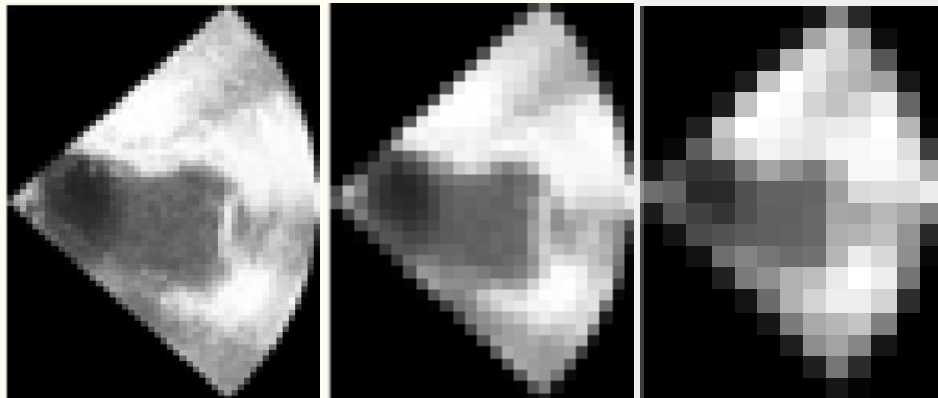
- Multi-scale (multi-resolution) training, where trained parameters in lower scale are used to initialize the higher scale training



Original

Pool-1 (stride 2)

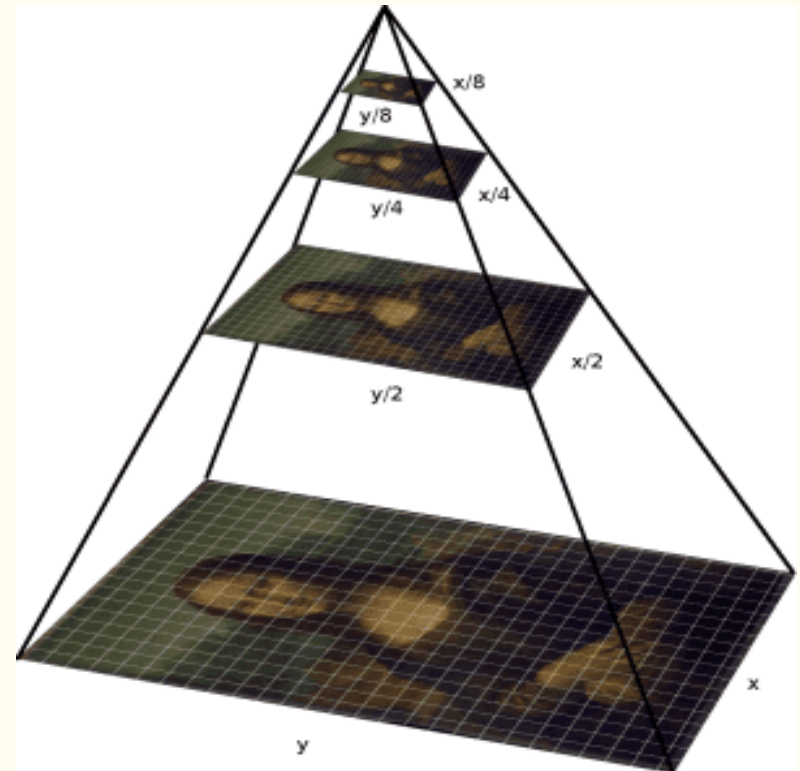
Pool-2 (stride 2)



Pool-3 (stride 2)

Pool-4 (stride 2)

Pool-5 (stride 2)



Results on CAMUS dataset

Scale 1
(112 × 144)

```
before_MSEMetric = 0.010041479021310806  
after_MSEMetric = 0.006580408196896315  
before_compute_meandice = [0.9668386  0.6937522  0.75969636]  
after_compute_meandice = [0.9774292  0.7890314  0.9059601]
```

Scale 2
(224 × 288)

```
before_MSEMetric = 0.009544618427753448  
after_MSEMetric = 0.005924441386014223  
before_compute_meandice = [0.9667753  0.69394   0.76024437]  
after_compute_meandice = [0.97944987  0.8144262  0.9186317 ]
```

Scale 3
(448 × 576)

```
before_MSEMetric = 0.009694118052721024  
after_MSEMetric = 0.0059749712236225605  
before_compute_meandice = [0.96685976  0.69459504  0.76026726]  
after_compute_meandice = [0.9799058  0.81560487  0.9229658 ]
```

Results (CAMUS 2D)

Model	MSE	Dice Score			Mean Dice ±std
		Background	Myo	LV	
Without Registration	0.00972	0.96678	0.69391	0.76046	0.80235± 0.05491
Vanilla-DLIR	0.0042	0.97352	0.74977	0.87523	0.88487± 0.03261
AC-DLIR	0.00598	0.97972	0.81437	0.91935	0.90303± 0.03447
Adv-DLIR	0.00533	0.97429	0.79278	0.86842	0.85733± 0.04129
AdvAC-DLIR	0.00589	0.98742	0.82751	0.93573	0.91689± 0.02596
MACMR	0.00489	0.98779	0.84871	0.95423	0.94245± 0.02474

Conclusion

- The clinical use of echo is still stuck with **2D**, so a more robust and precise automatic registration and segmentation framework is really needed
- Proposed **AdvAC** model outperforms all the previous experiments and thus proved to be the best model working in both the 2D and 3D dataset.
- Still, there is room for performance **improvement**.
- More annotated data for 3D will be needed for further performance improvement.

- **Annotate** more cases for 3D fetal data
- Apply the multi-resolution (**MACMR**) framework for 3D data
- Proceed with the 3D **segmentation** of heart chamber and myocardium
- Measure various identifiers as heart shapes, ejection fraction, volume etc. to perform disease **detection** and **classification** for fetal heart abnormalities

1. Wiputra, H., Chan, W.X., Foo, Y.Y., Ho, S., Yap, C.H., 2020. Cardiac motion estimation from medical images: a regularisation framework applied on pairwise image registration displacement fields. Scientific Reports 10.
2. Balakrishnan, Guha, et al. "VoxelMorph: a learning framework for deformable medical image registration." IEEE transactions on medical imaging 38.8 (2019): 1788-1800.
3. Hu, Yipeng, et al. "Label-driven weakly-supervised learning for multimodal deformable image registration." 2018 IEEE 15th International Symposium on Biomedical Imaging (ISBI 2018). IEEE, 2018.
4. Oktay, O., Ferrante, E. et al., 2017. Anatomically constrained neural networks (acnns): Application to cardiac image enhancement and segmentation. IEEE Transactions on Medical Imaging 37, 384–395
5. Leclerc, S., Smistad, E., et al., 2019. Deep learning for segmentation using an open large-scale dataset in 2d echocardiography. IEEE Transactions on Medical Imaging 38, 2198–2210. doi:10.1109/TMI.2019.2900516
6. Chen, X., Diaz-Pinto, A., Ravikumar, N., Frangi, A.F., 2021. Deep learning in medical image registration. Progress in Biomedical Engineering 3, 012003.
7. Li, Y., Sun, J., Tang, C.K., Shum, H., 2004. Lazy snapping. ACM SIGGRAPH 2004 Papers .
8. Ronneberger, O., Fischer, P., Brox, T., 2015. U-net: Convolutional networks for biomedical image segmentation. ArXivabs/1505.04597
9. Yan, P., Xu, S., Rastinehad, A.R., Wood, B.J., 2018. Adversarial image registration with application for mr and trus image fusion, in: MLMI@MICCAI.
10. Green, L., Chan, W.X., Ren, M., Mattar, C.N.Z., Lee, L.C., Yap, C.H., 2023. The dependency of fetal left ventricular biomechanics function on myocardium helix angle configuration. Biomechanics and modeling in mechanobiology 22, 629–643.
11. Izzo, R., Steinman, D.A., Manini, S., Faggiano, E., Antiga, L., 2018. The vascular modeling toolkit: A python library for the analysis of tubular structures in medical images. J. Open Source Softw. 3,745.
12. Lowekamp, B., gabehart, Blezek, D., Marstal, K., Ibanez, L., Chen, D., McCormick, M., Mueller, D., Johnson, H., Cole, D., Yaniv, Z., Posthuma, J., Beare, R., Gelas, A., aghayoor, Itong1130ztr, fsantini, adizhol, Subburam, K., Fillion-Robin, J.C., Anthony, Doria, D., King, B., 2016. kaspermarstal/simpleelastix: v0.10.0.

13. Nurmaini, Siti et al. "Deep Learning-Based Computer-Aided Fetal Echocardiography: Application to Heart Standard View Segmentation for Congenital Heart Defects Detection." *Sensors* (Basel, Switzerland) vol. 21,23 8007. 30 Nov. 2021, doi:10.3390/s21238007
14. <https://www.creatis.insa-lyon.fr/Challenge/CETUS/>
15. E. Smistad and F. Lindseth, "Real-time tracking of the left ventricle in 3D ultrasound using Kalman filter and mean value coordinates," in *Proc. MICCAI Challenge Echocardiogr. Three-Dimensional Ultrasound Segmentation (CETUS)*, Boston, MA, USA, 2014, pp. 65–72.
16. O. Oktay, W. Shi, K. Keraudren, J. Caballero, and D. Rueckert, "Learning shape representations for multi-atlas endocardium segmentation in 3D echo images," in *Proc. MICCAI Challenge Echocardiogr. Three-Dimensional Ultrasound Segmentation (CETUS)*, Boston, MA, USA, 2014, pp. 57–64.
17. Christoforos Sfakianakis, Georgios Simantiris, Georgios Tziritas: GUDU: Geometrically-constrained Ultrasound Data augmentation in U-Net for echocardiography semantic segmentation. *Biomed. Signal Process. Control.* 82: 104557 (2023)
18. Wei, Hongrong et al. "Temporal-Consistent Segmentation of Echocardiography with Co-learning from Appearance and Shape." *International Conference on Medical Image Computing and Computer-Assisted Intervention* (2020).
19. Hang Jung Ling, Damien Garcia, Olivier Bernard. Reaching intra-observer variability in 2-D echocardiographic image segmentation with a simple U-Net architecture. *IEEE International Ultrasonics Symposium (IUS)*, Oct 2022, Venice, Italy. (hal-03979523)
20. J. Zhang et al., "Dual-Branch TransV-Net for 3D Echocardiography Segmentation," in *IEEE Transactions on Industrial Informatics*, doi: 10.1109/TII.2023.3249904.

Thank you

Do you have any questions?
